High-resolution direct-comb spectrometer at 2.4 μm

E. Vicentini[1] on behalf of A. Rosina[2], M. Nobis[2], F. Canella[2],
Y. Wang[1], P. Laporta[1][2] and G. Galzerano[1][2]

[1] *Istituto di Fotonica e Nanotecnologie, CNR - Piazza Leonardo da Vinci 32, 20133 Milano, Italy*

[2] *Dipartimento di Fisica, Politecnico di Milano - Piazza Leonardo da Vinci 32, 20133 Milano, Italy*

Summary. — We present the implementation of a direct comb spectrometer capable of resolving the single-comb mode of a $\sim$200-MHz pulse repetition rate Cr:ZnSe mode-locked laser at 2.4 μm. The spectrometer is based on the combination of a scanning Fabry-Pérot micro-cavity resonator with a Finesse of 15000 and a diffraction reflecting grating. We demonstrate its application in high-precision spectroscopy of acetylene (C_2H_2) and deuterated methane (CDH_3) at 2.4 μm, over 3 THz bandwidth sampled at 200 MHz and with a frequency resolution of 100 kHz limited only by the comb mode linewidth.

1. – Introduction

Direct-frequency-comb spectroscopy (DFCS) is demonstrating to be a versatile diagnostic tool in many areas of science and technology thanks to its unique properties of ultrabroad bandwidth, high-speed detection, high sensitivity, high frequency resolution, and absolute frequency accuracy [1]. Achieving high resolution, which is obtained by resolving the single-comb mode, is fundamental for precision-spectroscopy applications where very narrow spectral features have to be detected over wide spectral bandwidths. Several DFCS methods have demonstrated so far the capability of resolving the comb mode spectral structure with frequency resolution ranging from tens of kilohertz to a few-gigahertz level, depending on optical bandwidth coverage and acquisition times [1]. Each of these DFCS methods is characterized by advantages and disadvantages in terms of complexity and the extension of the methodology to the most interesting spectral regions of the medium and far infrared where the fundamental vibrations and rotations of all molecules are present. For example, the dual-comb spectroscopy method, based on two comb sources with slightly detuned comb-line spacing [2], demonstrated excellent performance across a wide electromagnetic spectrum from visible to the far infrared

but at the price of using two comb sources and the need of some experimental tools to control the relative coherence between the two combs [3]. Alternative DFCS methods demonstrating single-comb tooth detection, such as Transform InfraRed (FTIR) [4] and Virtually Imaged Phased Array (VIPA) [5] spectroscopy techniques, showed some limitations, respectively, in terms of measurement speed (FTIR requires very long scanning arms) and spectral coverage (VIPA devices are not available in the mid and far infrared spectral regions).

In this paper, we present the implementation of a DFCS approach based on a scanning Fabry-Pérot micro-cavity resonator, SMART DFCS (Scanning Micro-cAvity ResonaTor DFCS) [6, 7], to the mid-infrared spectral region at around $2.4\,\mu$m using an ultrafast Cr:ZnSe laser comb. When applied to near-infrared spectral region, this method demonstrated state-of-the-art performance in a more flexible architecture of lower complexity. Here, we demonstrated that SMART can be easily extendible also to the mid-IR region of molecular fingerprinting. The characterization of the DFCS SMART method is performed using as spectroscopic target the absorption lines of acetylene molecules (^{12}C$_2$H$_2$ and ^{13}C$_2$H$_2$ isotopologs) and of deuterated methane (^{12}CDH$_3$) at around $2.45\,\mu$m.

2. – SMART spectrometer

In fig. 1, a scheme of the complete setup is presented. The scheme can be divided into two main sections: one is the frequency comb generation, based on a mode-locked
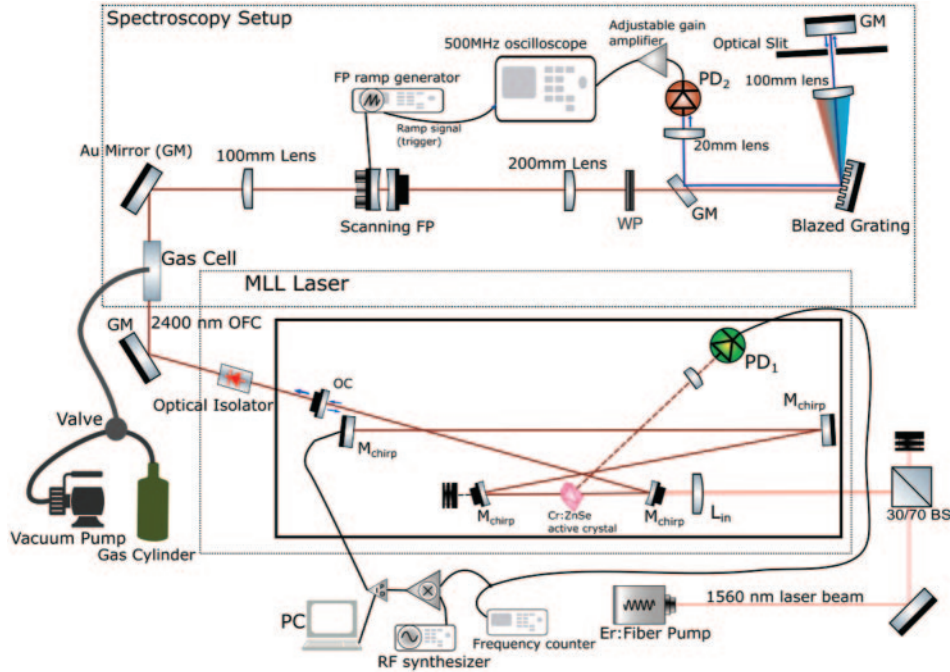

Fig. 1. – Schematic representation of the SMART setup divided in two parts. MLL laser: Cr:ZnSe mode lock laser. Spectroscopy Setup: scanning Fabry-Pérot microcavity resonator, filter and detector. FP: Fabry Pérot; GM: gold mirror; L: lens; M$_{chirp}$ chirped mirror; OC: output coupler; PD: photodetector; WP: $\lambda/2$ waveplate.

Cr:ZnSe laser and the electronics for its stabilization, the other is the spectroscopic section, constituted by the gas cell, the scanning Fabry-Pérot interferometer, the optical filter and the detection electronics. The optical frequency comb source is a homemade Kerr Lens mode-locked (KLM) Cr^{2+}:ZnSe laser [8]. The KLM provides pulses with a duration as short as 50 fs, a spectral bandwidth 6.2 THz (120 nm) centered at around 124 THz (2.4 μm), and an average output power of 110 mW. The pumping system of this laser is a commercial Er:fiber laser emitting at 1560 nm with a high-quality collimated single-mode output (1.5 mm beam radius, $M^2 = 1$) with a maximum CW power of 20 W. The operating power for mode-locking generation is around 3.5 W. The mode-locking pulse repetition frequency can be measured by a photodetector inside the laser box (PD1) which collects a leaked reflection of the active crystal. This signal is compared to a RF reference provided by a synthesizer in a fast phase discriminator. The phase discriminator output, adjusted by a proportional integrative derivative controller, is acting on one of the cavity mirrors mounted on a piezo-electric transducer to stabilize the pulse repetition frequency. After the Faraday isolator, a set of golden mirrors guides the mid infrared laser radiation through a 12-cm long glass cell, slightly tilted with respect to the beam to minimize undesired etalon effects. The beam, carrying now the spectroscopic information of the gas, is coupled by a 100-mm focal length plano-convex lens inside a scanning Fabry-Pérot (FP) micro-resonator with highly reflective mirrors and a nominal finesse at around 124 THz (2.4 μm) of 26000. One of the two FP mirrors is mounted on a piezo-electric transducer which can move the mirror up to 2 μm. The mirror movement is controlled by a periodic voltage ramp which scans back and forward the mirror in 300 ms. The cavity length change results in a continuous tuning of the cavity resonance frequency, equivalent to an optical spectrum analyser. The transmitted FP beam is then collimated by a 250 mm lens and sent to the filtering section of the spectrometer. The 4f "back-propagating" filter is composed of a diffraction grating (300 groves/mm) and an adjustable slit mounted on a linear stage. The back-propagated filtered beam is finally focused on a high-bandwidth, low-noise, homemade InGaAs photodiode by a 20 mm lens. The detector signal is then digitized by a 500 MHz bandwidth 12-bit oscilloscope.

3. – Spectroscopic results

The SMART method relies on the filtering capability of a scanning FP resonator that allows, in proper experimental conditions, the detection of the single tooth across the whole comb spectrum. For this purpose, the FP microresonator needs to be designed such that only one frequency comb mode can be resonant with the cavity itself. Two are the conditions to fulfill to achieve this result. First, the FP mode linewidth, $\delta\nu_{FP}$, needs to be narrower than the frequency comb mode spacing, the repetition rate f_{rep}, such that the single FP mode filters a single comb mode. Second, the FP mode periodicity, the free spectral range (FSR) needs to be larger than the spectral bandwidth of the comb source $\Delta\nu_{comb}$, such that only one FP mode is resonant with the frequency comb. These conditions can be fulfilled by a high-finesse micro-cavity. In the case of this experiment, with a frequency comb repetition frequency of 210 MHz and by considering a FP that filters with a factor of 100 the first neighbor comb mode, the minimum FP linewidth is $\delta\nu_{FP} = 2f_{rep}/\sqrt{100} = 40$ MHz. With a nominal microcavity finesse of 26000, this cavity linewidth can be achieved by setting the FSR at FSR = $F\delta\nu_{FP} = 1$ THz. This FSR is not sufficient to filter only one comb mode in the whole frequency comb bandwidth (more than 6 THz). For this reason, a second filtering stage is required, a stage with a frequency resolution better than 1 THz. This is a much easier condition to fulfill and a
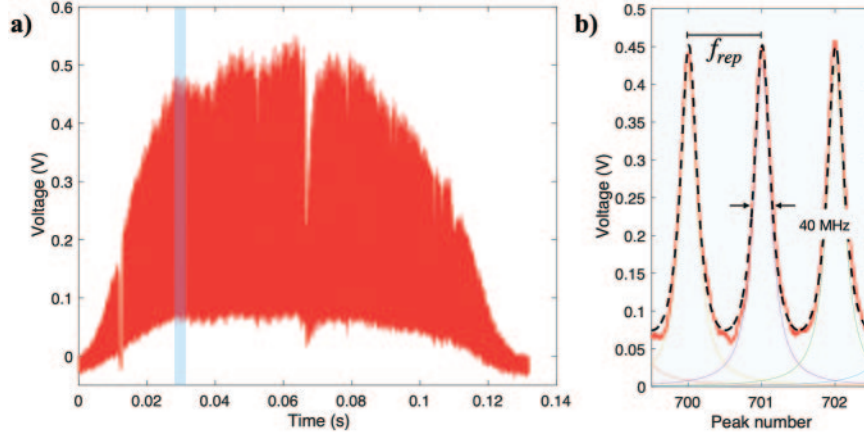
Fig. 2. – SMART acquisition. (a) Acquired data as a function of time. The acquired window spans ∼0.7 THz bandwidth and it contains ∼3500 comb lines. The deep modulation of the intensity is produced by the acetylene absorption. (b) Fit of 3 frequency comb modes (taken from the blue region of the panel). The red solid line is the acquired data; the color thin lines represent single mode contribution to the fit; the black dashed line represents the overall fit.

dispersion grating with an adjustable slit is used. Figure 2(a) shows the micro-resonator transmission *vs.* scanning time recorded at the output of the 4f filter. Using the comb repetition frequency value to calibrate the horizontal frequency axis, a FP microcavity linewidth of ∼40 MHz is measured, as shown in fig. 2(b), leading to a micro-cavity finesse of 18000.

Differently from previous implementation of the SMART spectrometer [6, 7], in this case the laser carrier envelop offset (CEO) frequency has not been stabilized. Even if this precludes the possibility to absolutely measure the frequencies of the comb teeth, a free-running CEO system strongly simplifies the setup allowing sufficient accuracy for many applications. In the present implementation, tabulated molecular absorptions reported in the HITRAN database [9] have been employed to calibrate the recorded spectra. One molecular absorption is used to assign the frequency of the closest comb mode and, starting from this fixed frequency, all the other comb modes are calculated by adding multiples of the repletion rate. To demonstrate the performance of the SMART method, we acquired high resolution spectra of isotopologs of methane and acetylene, in particular the CH_3D and the $^{13}C_2H_2$. Each gas sample was contained purified in a 12-cm long glass cell filled with a pressure of 500 mbar and 20 mbar, respectively for CH_3D and the $^{13}C_2H_2$.

The CH_3D molecule is reported in the HITRAN 2020 database [9], and the recorded spectrum can be directly calibrated and compared with it. Figure 3(a) shows the transmission spectrum over 500 GHz bandwidth measured in a single FP scan, with the 4-f filter centered around 122 THz. The acquired data have been numerically processed with a MATLAB script to retrieve the transmission spectra. The script finds the peak value of each comb mode and registers it as a sampling point of the spectrum. The frequency axis is successively constructed such that each point is equally spaced by the repetition frequency. Finally, the comb frequency offset is set such that one of the measured molecular absorptions best fits the HITRAN database line center. In the fitting analy-
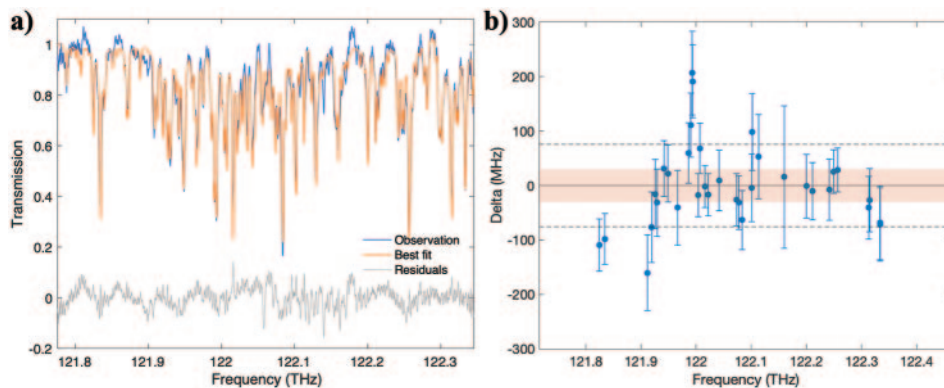
Fig. 3. – (a) Registration of CH$_3$D transmission spectrum. The observed transmission spectrum (blue solid line) has been fitted and compared with the HITRAN 2020 database (red solid line). The gray line represents the residuals of the fitting. (b) Line center difference between the fitted value and the HITRAN database line center frequency. Each fitted line center includes also the 95% confidence interval given by the fit. The black dashed lines represent the standard deviation of the line center differences. The red area represents the upper limit of HITRAN line center uncertainty (30 MHz).

sis of the spectrum, also the water absorption lines have been taken into consideration. Beside the water vapor present in the spectrometer path, the major contribution is coming from the water vapor present inside the laser cavity that strongly distorts the laser emission spectrum at around water vapour absorptions. To simplify the modelling of these spectral features, these profiles have been considered as a linear combination of real and imaginary part of the absorption profiles, which weights are fitted to the measurements. In the spectral window reported in fig. 3(a), two are the main water vapor absorptions to be considered, one at 122.13 THz and one at 122.30 THz. The retrieved line center frequencies of the measured CH$_3$D absorptions are reported in fig. 3(b). The results show a scattering of the line center positions with a standard deviation of 76 MHz, much higher than the line center accuracy reported in the HITRAN database for these rotovibrational lines (in the range from 3 to 30 MHz). This result is likely ascribed to a HITRAN database error. The repetition frequency was fixed during the experiment, ensuring a uniform line spacing of the frequency comb mode. The carrier envelop offset frequency is a slowly varying quantity, with variation of MHz per minute, so it can not strongly affect a 200 ms measurement time. The filtering action of the FP cavity can introduce instrumental distortion but, for the employed cavity linewidth, this effect is less than 1%, making also this effect negligible. The model employed for the fitting is a Voigt profile with all the coefficients (pressure shift, pressure broadening) set by the HITRAN database. While more sophisticated models of Voigt could be used, this should not affect much the line center frequency determination. The only possibility left is the HITRAN database, coefficients or reported line center frequency.

The second experiment is the spectroscopy of ^{13}C$_2$H$_2$. Since this molecule is not reported in the HITRAN 2020 database, we employed also an additional 10-cm gas cell filled with ^{12}C$_2$H$_2$ at a pressure of 10 mbar, to calibrate the recorded spectrum. The absorption spectra of ^{13}C$_2$H$_2$ were obtained by subtracting from the overall spectra recorded by the SMART DFCS those relating to the molecules of ^{12}C$_2$H$_2$ and water as computed
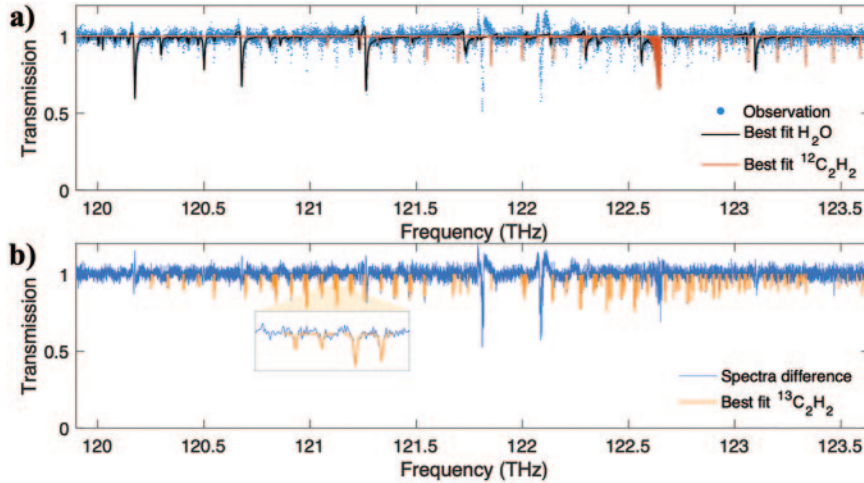
Fig. 4. – Spectroscopy of $^{13}C_2H_2$ and $^{12}C_2H_2$. (a) The measured transmission spectrum (blue dots) is characterised by the absorption of $^{13}C_2H_2$, $^{12}C_2H_2$ and H_2O. The HITRAN database allows subtracting the contribution of $^{12}C_2H_2$ (orange) and H_2O (black) from this spectrum. (b) The blue solid line represents the $^{13}C_2H_2$ spectrum obtained difference between the original transmission spectrum and the $^{12}C_2H_2$ and H_2O spectra. 135 different absorption lines have been identified and fitted to determine the line center frequency (orange solid line). The insert shows a detail of 4 absorption lines and their fit.

using the HITRAN database. Figure 4(a) shows the recorded spectrum over an optical bandwidth of $\sim$4 THz. This spectral region is larger than the FP FSR, approximately 0.5 THz, so several measurements have been used to compose the whole spectrum. Each of them has been obtained by moving the slit position of the 4-f filter. The composition of the spectrum has been made by using a common absorption between two different measurements. In this way, only one calibration is required and all the spectral points are equally spaced by the sampling frequency, the repetition rate. Figure 4(b) reports the retrieved transmission spectrum of the $^{13}C_2H_2$ molecule as obtained by the difference between the spectrum of fig. 4(a) and the reconstructed profiles of $^{12}C_2H_2$ and H_2O. It is worth noting that in the spectrum reported in fig. 4(b) 135 different absorption lines of $^{13}C_2H_2$ have been identified. Each of them has been fitted by a Lorentzian profile to determine the line center frequency, the area of the peak and the linewidth.

4. – Conclusion

We reported on the full characterization of a compact and versatile high-resolution direct-comb spectrometer in the mid-infrared spectral region at around $2.4\,\mu$m based on ultrafast Cr:ZnSe laser, a high-finesse scanning micro-resonator, and a low-resolution diffraction grating. In particular, high-resolution frequency spectroscopic investigations of acetylene (C_2H_2) and deuterated methane (CDH_3) over an optical bandwidth broader than 3.5 THz at around $2.4\,\mu$m have been performed with a frequency sampling of 200 MHz and a frequency resolution limited only by the comb mode linewidth.

* * *

REFERENCES

[1] PICQUÉ N. and HÄNSCH T. W., *Nat. Photon.*, **13** (2019) 146.
[2] KEILMANN F., GOHLE C. and HOLZWARTH R., *Opt. Lett.*, **29** (2004) 1542.
[3] MILLOT G., PITOIS S., YAN M., HOVHANNISYAN T., BENDAHMANE A., HÄNSCH T. W. and PICQUÉ N., *Nat. Photon.*, **10** (2016) 27.
[4] MEEK S. A., HIPKE A., GUELACHVILI G., HÄNSCH T. W. and PICQUÉ N., *Opt. Lett.*, **43** (2018) 162.
[5] DIDDAMS S. A., HOLLBERG L. and MBELE V., *Nature*, **445** (2007) 627.
[6] GAMBETTA A., CASSINERIO M., GATTI D., LAPORTA P. and GALZERANO G., *Sci. Rep.*, **6** (2016) 35541.
[7] VICENTINI E., GAMBETTA A., COLUCCELLI N., WANG Y., LAPORTA P. and GALZERANO G., *Phys. Rev. A*, **102** (2020) 033510.
[8] WANG Y., FERNANDEZ T. T., COLUCCELLI N., GAMBETTA A., LAPORTA P. and GALZERANO G., *Opt. Express*, **25** (2017) 25193.
[9] GORDON I. E. *et al.*, *J. Quant. Spectrosc. Radiat. Transf.*, **277** (2022) 107949.